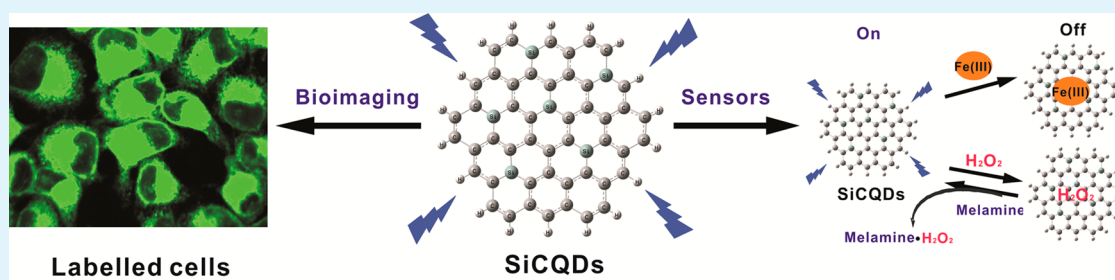# Si-Doped Carbon Quantum Dots: A Facile and General Preparation Strategy, Bioimaging Application, and Multifunctional Sensor

Zhaosheng Qian, Xiaoyue Shan, Lujing Chai, Juanjuan Ma, Jianrong Chen, and Hui Feng*

College of Chemistry and Life Science, Zhejiang Normal University, Jinhua 321004, China

S *Supporting Information*

ABSTRACT: Heteroatom doping of carbon quantum dots not only enables great improvement of fluorescence efficiency and tunability of fluorescence emission, but also provides active sites in carbon dots to broaden their application in sensor. Silicon as a biocompatible element offers a promising direction for doping of carbon quantum dots. Si-doped carbon quantum dots (SiCQDs) were synthesized through a facile and effective approach. The as-prepared Si-doped carbon quantum dots possess visible fluorescence with high quantum yield up to 19.2%, owing to fluorescence enhancement effect of introduced silicon atoms into carbon dots. The toxicity test on human Hela cells showed that SiCQDs have lower cellular toxicity than common CQDs, and bioimaging experiments clearly demonstrated their excellent biolabelling ability and outstanding performance in resistance to photobleaching. Strong fluorescence quenching effect of Fe(III) on SiCQDs can be used for its selective detection among general metal ions. Specific electron transfer between SiCQDs and hydrogen peroxide enables SiCQDs as a sensitive fluorescence sensing platform for hydrogen peroxide. The subsequent fluorescence recovery induced by removal of hydrogen peroxide from SiCQDs due to formation of the stable adducts between hydrogen peroxide and melamine was taken advantage of to construct effective sensor for melamine.

KEYWORDS: *Si-doped carbon quantum dots, bioimaging, hydrogen peroxide, melamine, sensor*

■ INTRODUCTION

Carbon quantum dots (CQDs), as novel and promising fluorescent materials, have attracted much attention due to their fascinating properties such as chemical inertness, lack of blinking, low toxicity, and excellent biocompatibility relative to traditional organic dyes and inorganic semiconductor quantum dots.[1,2] Much advance has been achieved in both CQDs preparation and applications.[3−7] A variety of methods including discharge, laser ablation, chemical and electrochemical oxidation, solvent-thermal, microwave-assistance, and dehydration of precursor were developed to synthesize CQDs.[8] To further improve the photoluminescence performance and enlarge application scope of CQDs, two kinds of modifications including surface functionalization and heteroatom doping were proposed. It has been proved that surface passivation of CQDs with polymers can largely increase their fluorescence quantum yields.[9,10] Current papers showed that surface functionalization with small organic amines can also lead to substantial fluorescence enhancement of functionalized CQDs,[11−14] and our group revealed the significant role of protonation of amino groups in the improvement of their fluorescence performance.[15] However, surface modification with polymers or small

organic molecules is usually complex to purify the functionalized CQDs, while these functionalized groups would occupy the position of functionals for specific analytical and sensor purpose.

Heteroatom doping into CQDs has been becoming a more powerful approach to improve the fluorescence properties of CQDs and broaden their applications in analysis and sensors. Nitrogen-doped CQDs (NCQDs) showed not only high luminescence performance but also high electrochemical activity.[16] N-doped CQDs with strong fluorescence through different methods including microwave-assistance, solvothermal synthesis and carbonization of precursors were prepared and applied in bioimaging.[17−19] Our recent work demonstrated that N-doped CQDs can act as a multifunctional fluorescence sensing platform for selective detection of Ag(I), Fe(III), and hydrogen peroxide.[20] Chandra et al. developed luminescent S-doped carbon dots as an emergent architecture for multimodal applications.[21] Our group proved that P-doped carbon

Scheme 1. Schematic Illustration of Detection Strategy of Melamine Based on SiCQDs
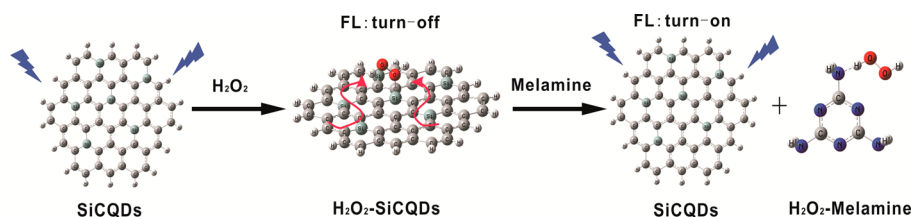
quantum dots can possess strong fluorescence, low toxicity, and excellent biolabelling to human Hela cells.[22] The doping of silicon (Si), which belongs to the same group as C, group IV, but strongly prefers sp[3]-like bonding, is considered to influence the electronic and structural properties of carbon-based material in a different way from that of N doping. As far as we know, not much is known about the properties of Si-doped CQDs and their photoluminescence performance. In view of the remarkable quantum-confinement and edge effects of carbon quantum dots, doping CQDs with Si atoms could alter their electronic characteristics and offer more active sites, thus producing new and unexpected properties and serving as novel nanodevices such as chemical sensors and toxic gas scrubbers.

Melamine (shorted for MA), with a chemical formula of $C_3H_6N_6$, is primarily used industrially in the production of filters, plastics, coatings, glues, laminates, and adhesives.[23] Because melamine contains a substantial amount of nitrogen (66% by mass), it had been added to dairy products to falsely enhance the measured protein content by unethical manufacturers. In recent years, melamine has been found in pet food, milk, infant formula, and other foods.[24] The melamine and related substances with toxic effects has been well-known worldwide for decades. Although melamine alone has low toxicity, the combination of melamine with cyanuric acid could form insoluble crystals in kidneys, thus causing the formation of kidney stones and even death.[25] It has been reported that there is an increasing number of kidney stones for thousands of infants in China, which has made melamine a worldwide food safety concern.[26] Thus, a variety of methods including capillary electrophoresis, high-performance liquid chromatography, liquid chromatography with mass spectrometry, LC with tandem, gas chromatography with mass spectrometry, nuclear magnetic resonance spectroscopy, vibrational spectroscopy, and chemiluminesence analysis have been developed for accurate detection of melamine, and were reviewed by Sun et al.[27] Because these methods often require expensive and complicated instruments, it pushes scientists to develop simple and new methods based on novel materials. Recent progress on detection of melamine focus on the utilization of inorganic nanomaterials including gold nanoparticles,[28] silver nanoparticles,[29] Fe_3O_4 magnetic nanoparticles,[30] $CuInS_2$ quantum dots,[31] and CdTe quantum dots.[32] However, their high synthesis expense, complicated procedure, and environmental incompatibility encourage analysts to discover cheap and green nanomaterials for the efficient determination of melamine in food that does not require complex procedure and expensive instruments.

In this work, we proposed a simple and efficient route to prepare silicon-doped carbon quantum dots (SiCQDs) with strong photoluminescence through a solvent-thermal reaction. The fluorescence is substantially enhanced through the doping of silicon relative to that of CQDs without silicon atoms, and quantum yield of SiCQDs is up to 19.2%. The toxicity and

bioimaging experiments showed that SiCQDs have low cell toxicity and excellent biolabelling ability, and have superiority in resistance to photobleaching. More importantly, H_2O_2 could substantially quench the fluorescence of SiCQDs through charge transfer between them. At the same time, the quenched fluorescence of SiCQDs can be recovered with the addition of melamine because melamine can form a stable adduct with H_2O_2 and thus remove H_2O_2 from surface of SiCQDs. The basic principle for detection of H_2O_2 and melamine based on Si-doped CQDs system is illustrated in Scheme 1. In the present work, the developed detection platform for H_2O_2 and melamine further exhibited the excellent properties of the as-prepared SiCQDs.

■ EXPERIMENTAL SECTION

Synthesis of Si-Doped Carbon Quantum Dots. Si-doped CQDs were synthesized through a solvent-thermal reaction using $SiCl_4$ as the silicon source and hydroquinone as the carbon precursor. The product with the ratio of 1:1 $SiCl_4$ and hydroquinone was obtained by placing 1.0 mL of $SiCl_4$, 0.97 g of hydroquinone, and 3.0 mL of acetone into a Teflon-lined stainless steel autoclave with 25 mL of capability, and then the mixture was heated at 200 °C for 2 h using a blast oven. After the autoclave cooled down to room temperature, the solution was condensed by rotary evaporation and the obtained product was Si-doped CQDs. To remove the extra reagent and small molecules, the as-prepared SiCQDs were further purified through dialysis (less than 3 kDa).

Characterization Methods. The morphologies of all samples were characterized by transmission electron microscopy (TEM), which was performed on a JEOL-2100F instrument with an accelerating voltage of 200 kV. Samples were prepared by dropping aqueous suspensions of the separated fractions of sample onto Cu TEM grids coated with a holey amorphous carbon film and following solvent evaporation in a dust protected atmosphere. The X-ray photoelectron spectroscopy analyses were conducted using a Kratos Axis ULTRA X-ray photoelectron spectrometer with a 165 nm hemisphereical electron energy analyzer. The incident radiation came from monochromatic Al X-ray (1486.6 eV) at 15 kV and 3 mA. Wide survey scans were taken at an analyzer pass energy of 160 eV over a 1400−0 eV binding energy with 1.0 eV step and a dwell time of 100 ms, while narrow multiplex higher resolution scans were performed at a pass energy of 20 eV with 0.05 eV step and a dwell time of 200 ms. The pressure in analysis chamber was less than 7.5×10^{-9} Torr during sample analysis. Atomic concentrations were calculated using Vision software and a Shirley baseline. The UV−Vis spectra were recorded on a PerkinElmer Lambda 950 spectrometer, in which the sample was dispersed in water after ultrasonication for 30 min. The photoluminescence spectra were conducted on a PerkinElmer LS-55 fluorescence spectrometer, and lifetimes were determined using a FLS920 fluorescence spectrophotometer. Raman spectra were recorded on a backscattered confocal configuration using a Renishaw RM1000 research laser Raman spectrometer with an excitation wavelength of 632.8 nm, a dwell time of 20 s, and a resolution of 1 cm^{-1}. Laser excitation was provided by a read He/Ne laser (632.8 nm, 1.96 eV), and the spectra were referenced to the silicon line at 520 cm^{-1}. The Fourier transform infrared spectroscopy (FT-IR) was
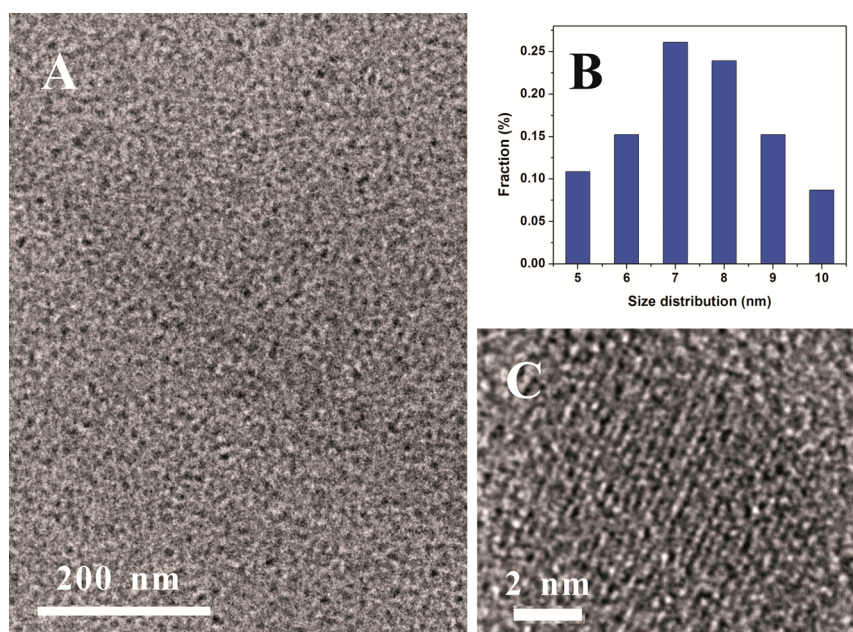
Figure 1. TEM image (A) and high-resolution TEM image (C) of as-prepared SiCQDs, and their size distribution (B).

carried out on a Thermo NEXUS 670 Fourier transform infrared spectrometer, in which the KBr plate method was used.

Determination of the Quantum Yields. Determination of the quantum yields of all samples was accomplished by comparison of the wavelength integrated intensity of sample to that of the standard quinine sulfate. The optical density was kept below 0.05 to avoid inner filter effects. The quantum yields of these oxidized products were calculated using

$$\Phi = \Phi_s[(I \cdot A_s \cdot n^2)/(I_s \cdot A \cdot n_s^2)]$$

where Φ is the quantum yield, I is the integrated intensity, A is the optical density, and n is the refractive index of the solvent. The subscript s refers to the standard reference of known quantum yield. Quinine sulfate was chosen as the standard, whose quantum yield is 0.577 and nearly constant for excitation wavelength from 200 to 400 nm. The slope method for determination of quantum yield was also used to confirm the obtained data.[33,34]

Cellular Toxicity Test. Human Hela cells (105 cells mL^{-1}) were cultivated in Dulbecco's modified Eagle's medium (DMEM) containing 10% fetal bovine serum and 100 μg mL^{-1} penicillin/streptomycin first for 12 h in an incubator (37 °C, 5% CO$_2$). Then suspensions of Si-doped CQDs with different doses were added, which kept final concentrations of Si-doped CQDs with 0, 25, 50, 75, and 100 μg mL^{-1}, respectively. The cells were cultivated for 24 h and then 20 μL of 5 mg mL^{-1} MTT solution was added to every cell well. After the cells were further incubated for 4 h, the culture medium was removed and then 150 μL of DMSO was added. The resulting mixture was mixed for 15 min at room temperature without light. The optical density (OD) of the mixture was measured at 570 nm. The OD values were determined using a Thermo Scientific Multiskan spectrum microplate spectrophotometer. The cell viability was estimated according to the following equation

$$\text{cell viability (\%)} = \text{OD}_{\text{treated}}/\text{OD}_{\text{control}} \times 100\%$$

where OD$_{\text{control}}$ was obtained in the absence of SiCQDs and OD$_{\text{treated}}$ was obtained in the presence of SiCQDs.

Cellular Imaging. The human Hela cells were cultivated for 12 h in a culture medium containing DMEM supplemented with 10% fetal bovine serum and 100 μg mL^{-1} penicillin/streptomycin. Suspensions of Si-doped CQDs from the stock solution were prepared with Dulbecco's phosphate buffer saline (DPBS). The suspension was added to the well of a chamber slide, and the final concentration of SiCQDs was 50 μg mL^{-1}, followed by incubating at 37 °C in a 5%

CO$_2$ incubator for 24 h. Prior to inspection with a Leica laser scanning confocal microscope, the excess SiCQDs were removed by washing three times with warm DPBS. The fluorescence images were obtained at the excitation wavelength of 355 nm.

Determination of Fe(III), H$_2$O$_2$, and Melamine. All fluorescence spectra were recorded on a PerkinElmer LS-55 luminescence spectrometer in the buffer solution at pH 7.4. The following metal ions were chosen to evaluate the influence of metal ions on fluorescence of SiCQDs, and assess the selectivity of Fe(III) based on fluorescence variation: Na$^+$, K$^+$, Mg^{2+}, Zn^{2+}, Ni^{2+}, Cu^{2+}, Mn^{2+}, Co^{2+}, Pb^{2+}, Cd^{2+}, Ag$^+$, Hg^{2+}, Fe^{2+}, Al^{3+}, and Fe^{3+}. To eliminate the pH effect induced by metal ions, all experiments were performed at pH 1.0. For selectivity of the SiCQDs toward metal ions, the concentrations of the chosen metal ions were 0.01 M. For the quantitative measurement of Fe(III), a series of Fe$_2$(SO$_4$)$_3$ and SiCQDs solutions were prepared, in which the concentration of SiCQDs was kept identical and the concentrations of Fe(III) varied from 4.0×10^{-6} to 1.2×10^{-4} M. The quenching effect of H$_2$O$_2$ on the fluorescence of SiCQDs was conducted as follows: 2.0 mL of SiCQDs suspension in ethanol and 1.0 mL of phosphate buffer solution (PBS, pH 7.4) were mixed. Then, a series of H$_2$O$_2$ solutions with different concentrations were added into the proceeding solutions, which were finally diluted to 4.0 mL with butter solution. Thus, a series of mixed solutions including SiCQDs with the same concentration and H$_2$O$_2$ with different concentrations were prepared, and then their fluorescence intensities were determined using a fluorescence spectrometer after 5 min of sonication and another 5 min of standing. The detection of melamine was carried out as follows: 2.0 mL of SiCQDs suspension in ethanol, 1.0 mL of phosphate buffer solution (PBS, pH 7.4), and 0.5 mM of H$_2$O$_2$ were mixed. Then, a series of melamine solutions with different concentrations ranging from 0.1 to 50.0 μM were added into the above mixed solutions, and the resulted solutions were finally diluted to 4.0 mL. Their fluorescence intensities were determined using a fluorescence spectrometer after 5 min of mixing.

■ RESULTS AND DISCUSSION

Preparation and Characterization of SiCQDs. The Si-doped carbon quantum dots (SiCQDs) were synthesized by solvothermal reaction between silicon chloride and carbon precursor including hydroquinone under 200 °C in a Teflon-lined vessel. The as-prepared SiCQDs present strong blue fluorescence. To explore the role of doped silicon in the CQDs,
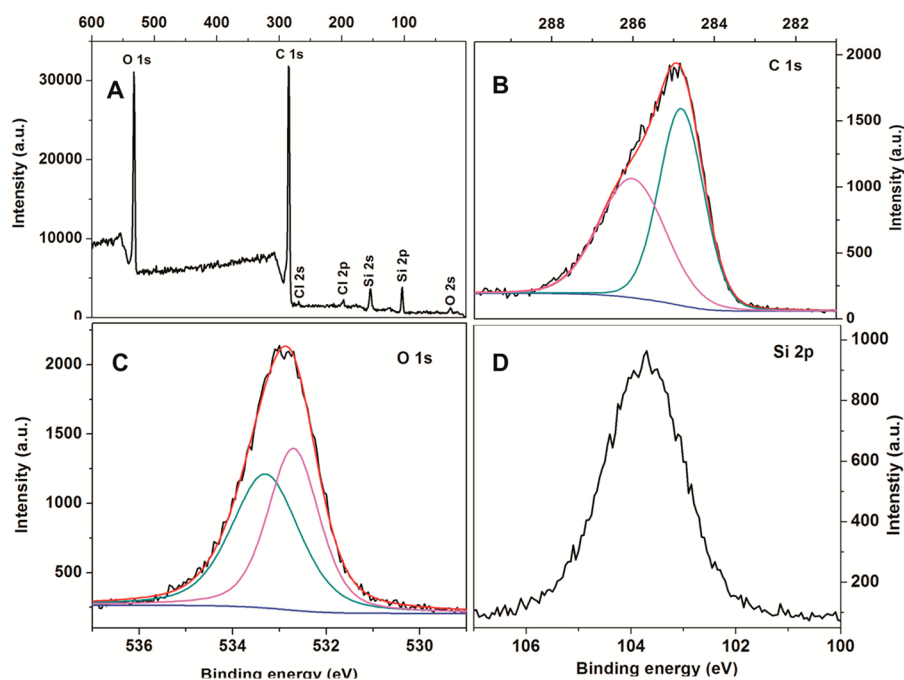
Figure 2. Wide scan XPS spectrum of SiCQDs (A), and the enlarged regions for C 1s (B), O 1s (C), and Si 2p (D) of SiCQDs.

we compared the size, composition, and fluorescence properties between SiCQDs and pristine CQDs reported in our previous paper. Figure 1 shows typical TEM images of SiCQDs and their size distribution. The size distribution showed that average size of SiCQDs is 7 ± 2 nm whereas pristine CQDs have a smaller size of 3−5 nm. HR-TEM image of SiCQDs in Figure 1C indicated SiCQDs also possess crystalline lattice structures similar to CQDs. The spacing of adjacent lattice planes is about 3.4 Å, close to that of phosphorus-doped CQDs (PCQDs) (3.0 Å)[22] and nitrogen-doped CQDs (NCQDs) (3.2 Å).[18,19] The thickness distribution of SiCQDs was characterized by atomic force microscopy (AFM) measurements. Figure S2 (Supporting Information) shows the representative AFM image of the sample. Thickness distribution reveals that the thickness of SiCQDs varies from 4.0 to 6.0 nm, close to those of NCQDs reported previously.[20]

The compositions of SiCQDs samples were further analyzed by X-ray photoelectron spectroscopy (XPS). The XPS spectrum of SiCQDs in Figure 2A displayed four predominant peaks including C 1s peak at 284.8 eV, O 1s peak at 532.8 eV, Si 2s peak at 153.9 eV, and Si 2p peak at 103.6 eV,[35] indicating the successful doping of Si atoms into carbon dots. Except for these dominant peaks, small Cl 2s and Cl 2p peaks at 269.0 and 196.9 eV from C—Cl in SiCQDs were also observed, indicating a small amount of chlorine atoms was introduced into carbon dots. Figure 2B shows the C 1s peak mainly consists of two subpeaks at 284.8 and 286.0 eV, which can be assigned to C=C and C—O bonds, respectively, implying a lack of Si—C bonds in SiCQDs. As shown in Figure 2C, O 1s peak is composed of two subpeaks at 533.3 and 532.7 eV, which are from O—C and O—Si groups, respectively.[35] The Si 2p peak at 103.7 eV comfirmed the dominant form of silicon as Si—O group in SiCQDs. The elemental analysis determined by XPS in Table 1 displayed that the SiCQDs are composed of 60.1% C, 27.3% O, 11.0% Si, and 1.6% Cl. Compared with the composition of pristine CQDs, the contents of carbon, oxygen, and chlorine in SiCQDs were not largely changed except for

Table 1. Concentration of C, O, Cl and Si in the SiCQDs and CQDs Samples As Determined by XPS

samples	C [wt %]	O [wt %]	Cl [wt %]	Si [wt %]
SiCQDs	60.1	27.3	1.6	11.0
CQDs[a]	67.8	26.8	5.4	

[a]The data for CQDs is from Ref 22.

the incorporation of considerable amount of silicon atoms. The FT-IR spectrum of SiCQDs shown in Figure S3 (Supporting Information) clearly demonstrated the vibrational peaks at 1102, 818, and 465 cm^{-1}, which are originated from vibrations of Si—O bond in SiCQDs, consistent with XPS results. The comparison of Raman shift between SiCQDs and CQDs (Figure S4, Supporting Information) showed that both of them possess the D band at approximately 1350 cm^{-1} from the disorder in sp^2-hybridized carbon system and the G band at about 1580 cm^{-1} from the stretching of C—C bond in sp^2 carbon system, but their D/G ratios have much difference, indicating the incorporation of silicon atoms substantially increases the disorder of crystalline strucure in SiCQDs.

Fluorescence of SiCQDs and Their Application in Bioimaging. The as-prepared SiCQDs are easily soluble in ethanol and sparingly soluble in water. Both of their suspensions in ethanol and water exhibit strong blue fluorescence, as shown in Figure 3A inset. Figure 3A presents the comparison of emission spectra among CQDs, SiCQDs, and PCQDs. The SiCQDs have a broad emission band centered at 382 nm, and their emission is largely blue-shifted relative to that of CQDs, which emit the light of 440 nm. This blue-shift of emission for SiCQDs results from the introduction of large amounts of Si—O groups into conjugated carbon structure, which is similar to the role of P—O group in PCQDs on emission. Figure 3B depicted the time-resolved fluorescence decay curves of CQDs, SiCQDs, and PCQDs. These curves imply that CQDs have a longer lifetime than those of SiCQDs and PCQDs. This is verified by their lifetime data shown in
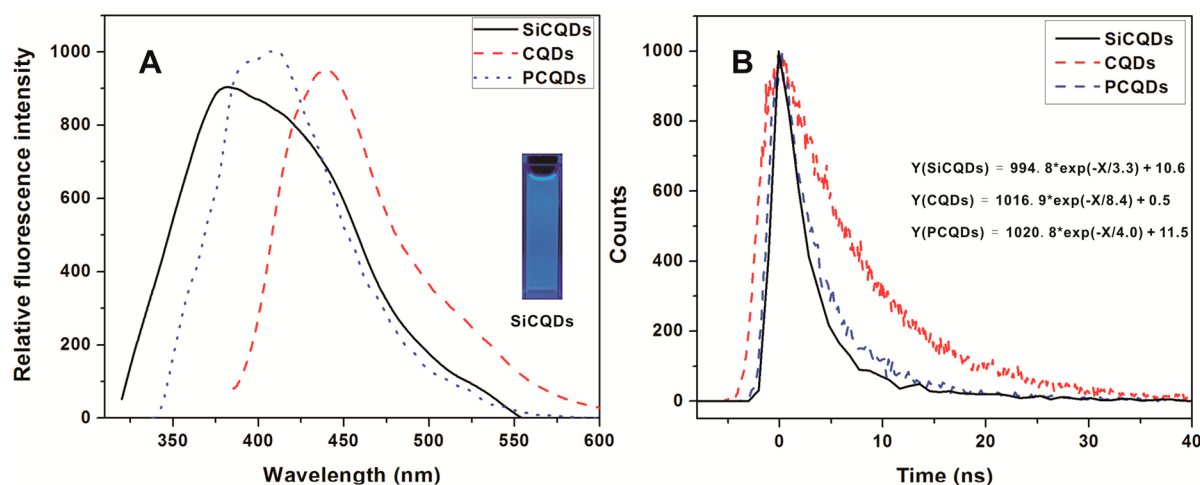
Figure 3. Fluorescence emission spectra of SiCQDs, pristine CQD, and PCQDs at the excitation wavelength of 300, 368, and 372 nm, respectively (A), and their time-resolved fluorescence decay curves (B). The data for CQDs and PCQDs are from ref 22. Panel A inset: fluorescence images of SiCQDs. Panel B inset: the fitting equations for their decay curves.

Table 2. The large lifetime difference between SiCQDs and CQDs further proved that the silicon atoms were incorporated

Table 2. Fluorescence Quantum Yields and Lifetimes of CQDs, PCQDs, and SiCQDs

sample	λ_{ex} [nm]	λ_{em} [nm]	$\Phi_f{}^a$ [%]	τ^b [ns]
CQDs[c,d]	368	440	3.4	8.4
PCQDs[c,d]	372	410	25.1	4.0
SiCQDs	300	382	19.2	3.3

[a]The fluorescence quantum yields. [b]The average lifetimes. [c,d]From ref 22.

into carbon dots, and the Si-doped carbon dots showed distinct fluorescence behavior from pristine CQDs. More importantly, the quantum yield of SiCQDs is up to 0.19, close to that of PCQDs (0.25) and much higher than that of CQDs (0.034),[22] which clearly demonstrated that the incorporation of silicon can substantially enhance the fluorescence of carbon dots. Similar with carbon nanodots, SiCQDs also have excitation-wavelength-dependent PL properties, as illustrated in Figure S6

(Supporting Information), indicating their fluorescence can be tuned with different excitation wavelengths. As stated in our recent paper on PCQDs,[22] the fluorescence enhancement mechanism by heteroatoms such as nitrogen, phophrous, and silicon remains unclear because the fluorescence nature of carbon dots is still a controversy until now. Our group has systematically investigated the fluorescence of carbon-based nanomaterials through experimental and theoretical approaches and compared the different proposal on the nature of fluorescence of carbon nanodots.[36] It is favorable for the defects mechanism and isolated sp^2 conjugated carbon cluster mechanism to explain the fluorescence enhancement by heteroatoms. The fluorescence enhancement can be originated from more isolated sp^2 conjugated carbon clusters resulting from the incoporation of a large amount of silicon atoms. Thus, the introduction of a great deal of silicon atoms results in the formation of more isolated sp^2 conjugated carbon clusters as fluorophores, leading to the enhancement of fluorescence intensity. However, another possibility cannot be excluded: the introduction of many silicon atoms into carbon dots leads to
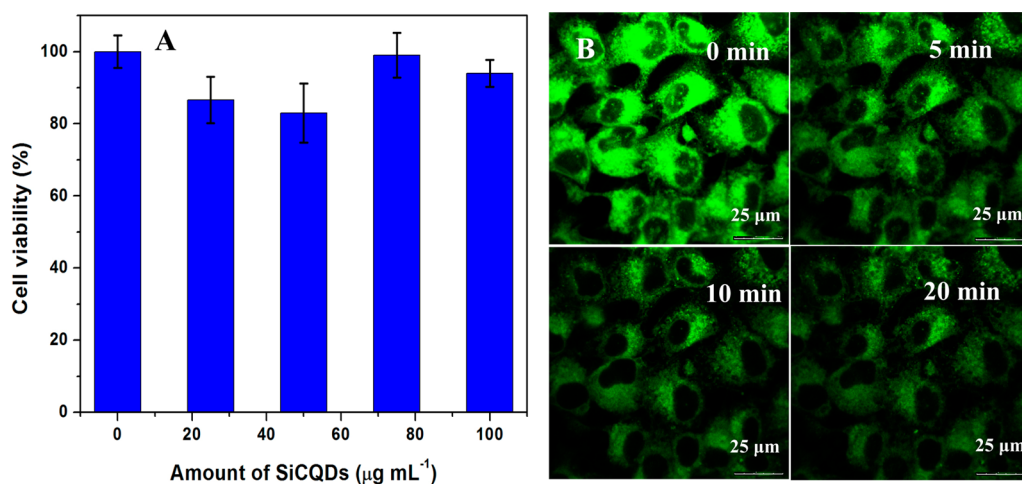

Figure 4. Effect of SiCQDs on human Hela cells (A) and laser scanning confocal microscopy images of human Hela cells labeled by SiCQDs (B) with different exposure time to UV light.
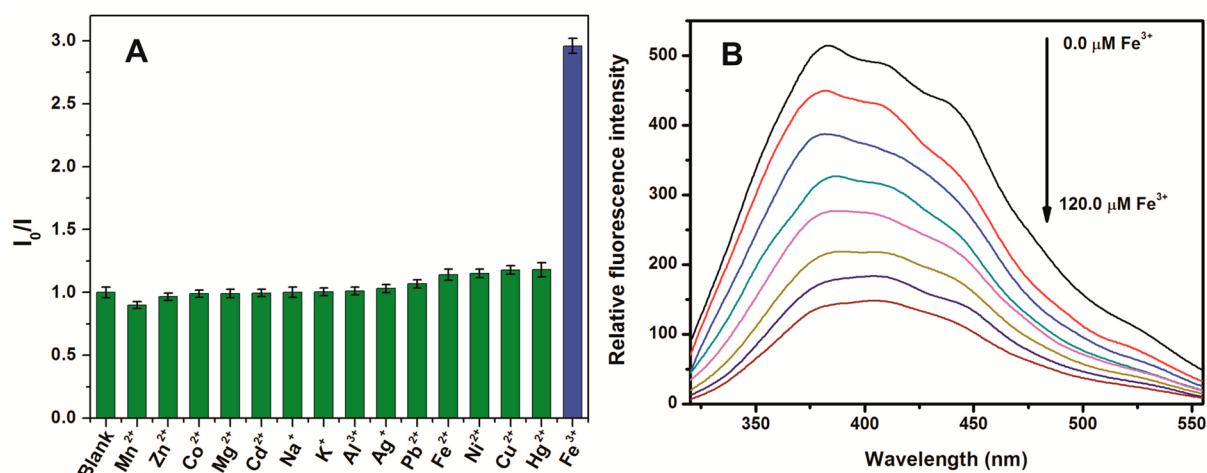
Figure 5. Influence of different metal ions on the fluorescence of SiCQDs (A) and fluorescence intensity dependence on concentration of Fe(III) (B). I_0 represents the fluorescence intensity of SiCQDs and I represents the fluorescence intensity of a mixture of metal ions and SiCQDs.
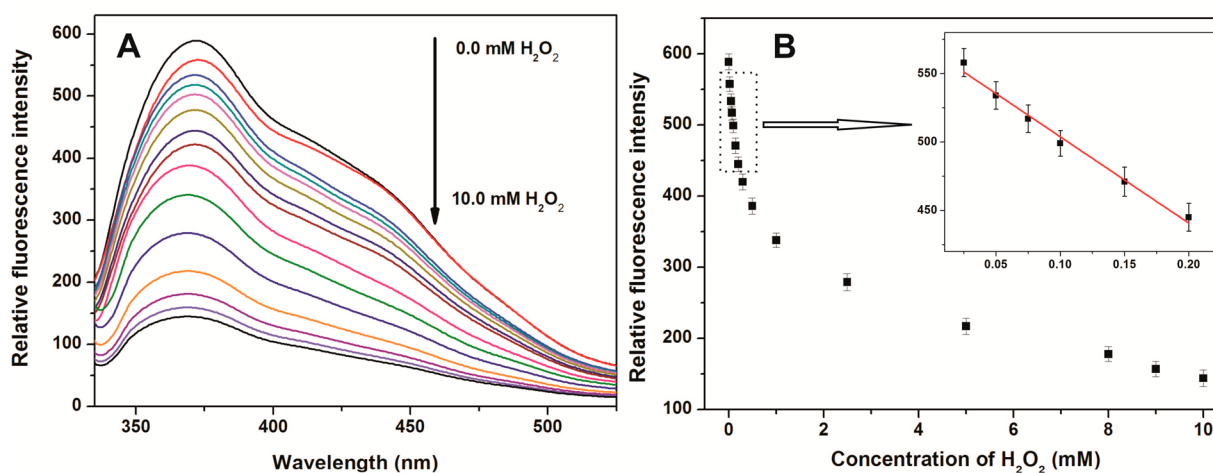

Figure 6. (A) Fluorescence spectra of SiCQDs with varying concentrations of H_2O_2. (B) Fluorescence intensity dependence on varying amounts of H_2O_2. Inset: linear relationship between fluorescence intensity and concentration of H_2O_2.

the formation of more defect sites in the large conjugated carbon structure, thus giving rise to stronger fluorescence.

To assess the possible celluar toxicity brought by doped Si atoms, in vitro cytotoxicity of Si-doped CQDs was evaluated with human Hela cells by methylthiazolydiphenyltetrazolium bromide (MTT) assay, as shown in Figure 4A. Results suggested that SiCQDs showed low toxicity to human Hela cells with a cell viability of higher than 80% when their contents remain below 100 μg mL^{-1}. Their toxicity to human Hela cells is comparable to those of CQDs and NCQDs,[20] and lower than that of PCQDs,[22] indicating the doping of Si atoms have no remarkable influence on cell toxicity of CQDs. We also tested their ability to label the cells as shown in Figure 4B. It can be seen that SiCQDs easily went into the cytoplasm through the cell membrane and clearly labeled the area of the cytoplasm. The fluoresence of the labelled area with SiCQDs is much stronger than that of CQDs, and comparable to that of PCQDs and NCQDs due to their higher emission efficiency.[20,22] After 20 min of exposure to UV light, the fluorescence of SiCQDs remains bright, clearly demonstrating the strong resistance ability of SiCQDs to photobleaching. Compared with those of CQDs and NCQDs, SiCQDs have superiority in resistance to photobleaching, thus in bioimaging.[20]

Selective Detection of Fe(III), H_2O_2, and Melamine Based on SiCQDs. Our previous research indicated that fluorescent carbon nanomaterials can be employed to detect metal ions based on their distinct effect on the fluorescence.[37−39] Our recent paper reported that NCQDs can act as a multifunctional fluorescence sensing platform for detection of Ag(I) and Fe(III) because Ag(I) can largely enhance the fluorescence while Fe(III) can strongly quench the fluorescence.[20] Therefore, we evaluated the influence of different metal ions on fluorescence of SiCQDs as shown in Figure 5A. Fifteen metal ions including Na$^+$, K$^+$, Mg^{2+}, Zn^{2+}, Ni^{2+}, Cu^{2+}, Mn^{2+}, Co^{2+}, Pb^{2+}, Cd^{2+}, Ag$^+$, Hg^{2+}, Fe$^{2,+}$ Al^{3+}, and Fe^{3+} were chosen to assess the impact on fluorescence intensity of SiCQDs. It is found that SiCQDs can selectively detect Fe^{3+} among these cations because of the strongest quenching effect of Fe^{3+} on the fluorescence. Figure 5B shows that the fluorescence intensity linearly decreased with the concentration of Fe^{3+}, implying the capability of SiCQDs to quantitative detection of Fe^{3+}. However, the selectivity coefficient I_0/I for Fe(III) on SiCQDs is only about 3, which is much lower than that on NCQDs (40). This large difference may be because NCQDs can form stable complex with Fe^{3+} with nitrogen sites
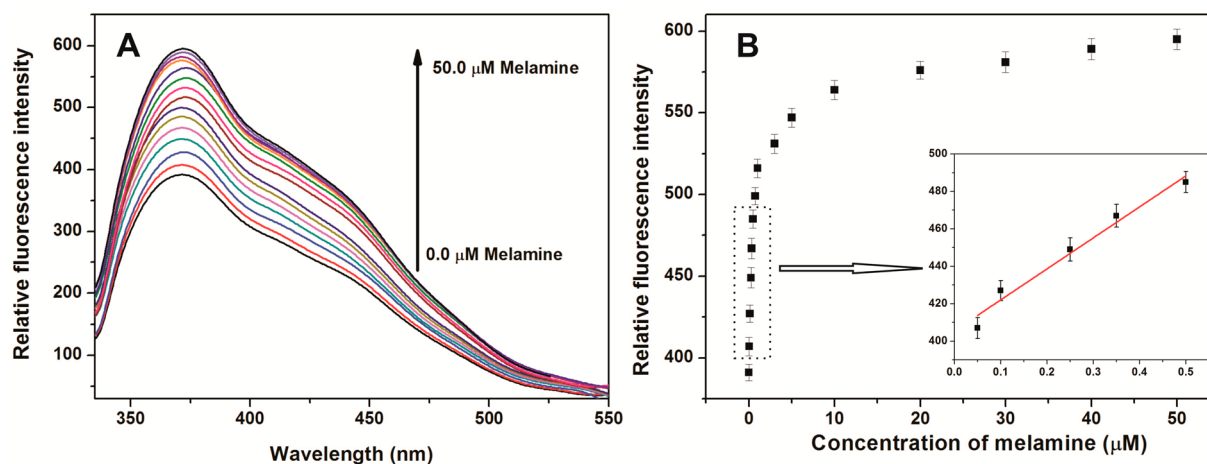
Figure 7. (A) Recovered fluorescence spectra of SiCQDs with varying amounts of melamine after the addition of H_2O_2 (0.5 mM). (B) Recovered fluorescence intensity dependence on varying amounts of melamine. Inset: linear relationship between fluorescence intensity and concentration of melamine.

Table 3. Comparison among Fluorescent Nanomaterials-Based Methods for Detection of Melamine

materials	detection limit (mol L^{-1})	concentration range (mol L^{-1})	response time (min)	ref
Au nanoparticles	6.1×10^{-10}	$8.0 \times 10^{-10} - 8.0 \times 10^{-8}$	40	42
Au nanoparticles	1.0×10^{-9}	$1.0 \times 10^{-7} - 4.0 \times 10^{-6}$	5	43
CdTe QDs	4.0×10^{-8}	$7.9 \times 10^{-8} - 7.9 \times 10^{-7}$	10	32
CdTe@SiO$_2$	8.9×10^{-10}	$7.5 \times 10^{-9} - 3.5 \times 10^{-7}$	30	44
CuInS$_2$ QDs	5.0×10^{-9}	$1.0 \times 10^{-8} - 1.0 \times 10^{-5}$	20	31
CdS QDs	1.0×10^{-9}	$2.0 \times 10^{-9} - 5.0 \times 10^{-5}$	20	45
SiCQDs	8.0×10^{-9}	$5.0 \times 10^{-8} - 5.0 \times 10^{-7}$	5	This work

whereas SiCQDs can only physically absorb Fe^{3+} on the surface.

Interestingly, it is found that the fluorescence of SiCQDs can be substantially quenched by H_2O_2 whereas only very small decreases can be observed for CQDs, indicating introduced silicon atoms play a key role in the fluorescence quenching by H_2O_2. It is reported that hydrogen peroxide can also quench the fluorescence of CdTe quantum dots (CdTe QDs) and Si quantum dots (SiQDs).[40,41] For the CdTe QDs, it is assumed that electron-transfer reaction between CdTe QDs and H_2O_2 leads to O_2, which, as a good electron acceptor, in turn, lies in electron/hole traps on QDs, thus forming the nonfluorescent QDs anion, resulting in the fluorescence quenching.[40] For SiQDs, it is presumed that active oxygen species of H_2O_2 can capture electrons at the conduction bands of SiQDs, thus inhibiting the radiative recombination of photoinduced electrons and holes, leading to reduced fluorescence.[41] Both the proceeding proposals involved the production of active O_2 through electron-transfer reaction from H_2O_2. However, the quenching mechanism by active oxygen species produced by H_2O_2 could be excluded for SiCQDs because the fluorescence quenched by H_2O_2 can be nearly completely recovered by addition of melamine. The recovery of the fluorescence is attributed to removal of H_2O_2 from surface of SiCQDs by melamine to form stable adduct between H_2O_2 and melamine. Therefore, it is reasonable to assume that H_2O_2 can easily attach on the surface of SiCQDs through silicon sites, and subsequent electron transfer between SiCQDs and H_2O_2 leads to reduced fluorescence, which can be recovered through capture of H_2O_2 by melamine. Upon this special fluorescence "on−off−on" property, we constructed the fluorescence sensing system for detection of H_2O_2 and melamine. The fluorescence

response of SiCQDs to H_2O_2 concentration is shown in Figure 6A. Upon stepwise addition of H_2O_2, the PL intensity of SiCQDs gradually decreased. The fluorescence remains nearly constant when the added H_2O_2 is over 10.0 mM, indicating surface of SiCQDs is saturated with hydrogen peroxide molecules. The fluorescence is inversely linear with the concentration of H_2O_2 from 0.025−0.2 mM shown in Figure 6B. The detection limit of this method for H_2O_2 is 2.1 μM, which is better than that based on SiQDs.[41]

As mentioned previously, the quenched fluorescence of the SiCQDs by H_2O_2 could be recovered upon the addition of melamine. The fluorescence response of this system was evaluated by adding different concentrations of melamine in pH 7.4 buffer solutions at 37 °C for 20 min. Figure S8 (Supporting Information) shows that the optimum response time for fluorescence recovery of SiCQDs with melamine is 5 min. It can be seen from Figure 7A that the fluorescence intensity of SiCQDs quenched by H_2O_2 could be gradually recovered upon the addition of different concentrations of melamine. The fluorescence of SiCQDs nearly completely recovered when the added melamine is up to 20 μM. Figure 7B shows a good linear relationship between the recovered fluorescence and concentration of melamine in the range of 0.05−0.5 μM. The detection limit was determined to be 8.0 nM. Table 3 summarizes the fluorescent nanomaterials-based methods for detection of melamine. These methods employed expensive inorganic nanomaterials,[31,32,42−45] but we utilized cheap and environmentally friendly carbon nanodots to detect melamine for the first time. The detection limit and linear concentration range of our method are comparable with those of most reported methods. More importantly, our method possesses

much shorter response time (only 5 min), which is better than most of the other methods.[31,32,42−45]

CONCLUSION

In summary, we developed a simple and effective method to synthesize Si-doped carbon quantum dots with high efficient fluorescence. The doping of Si atoms can tune the emission band and substantially improve the emission efficiency of carbon dots. The toxicity and bioimaging experiments showed that Si-doped CQDs have low cell toxicity, excellent biolabelling ability, and good resistance to photobleaching. The Si-doped CQDs exhibit an excellent and multifunctional sensing performance in determination of Fe(III), H_2O_2, and melamine. The selective detection of hydrogen peroxide was achieved through unique electron transfer between SiCQDs and hydrogen peroxide by silicon sites. The specific fluorescence recovery induced by formation of the adduct between hydrogen peroxide and melamine was taken advantage of to realize the sensitive quantitation of melamine. More notably, this work clearly shows that Si-doped CQDs can serve as a promising platform for constructing practical fluorescent nanosensors, and the proposed detection platform may have a great potential for quantitatively monitoring the intracellular species.

ASSOCIATED CONTENT

ⓈSupporting Information

UV−Visible spectrum, FT-IR spectrum, Raman spectra, atomic force microscopy image, the fluorescence excitation and emission spectra of SiCQDs and CQDs, laser scanning confocal microscopy images of human Hela cells without SiCQDs, and response time of fluorescence recovery of SiCQDs. This material is available free of charge via the Internet at http://pubs.acs.org.

AUTHOR INFORMATION

Corresponding Author
*H. Feng. E-mail: fenghui@zjnu.cn. Tel: +86-579-82282269. Fax: +86-579-82282269.

Notes
The authors declare no competing financial interest.

ACKNOWLEDGMENTS

REFERENCES

(1) Baker, S. N.; Baker, G. A. Luminescent Carbon Nanodots: Emergent Nanolights. *Angew. Chem., Int. Ed.* **2010**, *49*, 6726−6744.

(2) Zhu, S.; Tang, S.; Zhang, J.; Yang, B. Control the Size and Surface Chemistry of Graphene for the Rising Fluorescent Materials. *Chem. Commun. (Cambridge, U. K.)* **2012**, *48*, 4527−4539.

(3) Shen, J. H.; Zhu, Y. H.; Yang, X. L.; Li, C. Z. Graphene Quantum dots: Emergent Nanolights for Bioimaging, Sensors, Catalysis and Photovoltaic Devices. *Chem. Commun. (Cambridge, U. K.)* **2012**, *48*, 3686−3699.

(4) Li, H. T.; Kang, Z. H.; Liu, Y.; Lee, S.-T. Carbon Nanodots: Synthesis, Properties and Applications. *J. Mater. Chem.* **2012**, *22*, 24230−24353.

(5) Zheng, L.; Chi, Y.; Dong, Y.; Lin, J.; Wang, B. Electrochemiluminescence of Water-Soluble Carbon Nanocrystals Released Electrochemically from Graphite. *J. Am. Chem. Soc.* **2009**, *131*, 4564−4565.

(6) Dong, Y.; Zhou, N.; Lin, X.; Lin, J.; Chi, Y.; Chen, G. Extraction of Electrochemiluminescent Oxidized Carbon Quantum Dots from Activated Carbon. *Chem. Mater.* **2010**, *22*, 5895−5899.

(7) Yang, S.; Liang, J.; Luo, S.; Liu, C.; Tang, Y. Supersensitive Detection of Cholorinated Phenols by Multiple Amplification Electrochemiluminescence Sensing Based on Carbon Quantum dots/Graphene. *Anal. Chem.* **2013**, *85*, 7720−7725.

(8) Li, L.; Wu, G.; Yang, G.; Peng, J.; Zhao, J.; Zhu, J. Focusing on Luminescent Graphene Quantum Dots: Current Status and Future Perspectives. *Nanoscale* **2013**, *5*, 4015−4039.

(9) Sun, Y.-P.; Zhou, B.; Lin, Y.; Wang, W.; Fernando, K. A. S.; Pathak, P.; Meziani, M. J.; Harruff, B. A.; Wang, X.; Wang, H. F.; Luo, P. G.; Yang, H.; Kose, M. E.; Chen, B. L.; Veca, L. M.; Xie, S.-Y. Quantum-Sized Carbon Dots for Bright and Colorful Photoluminescence. *J. Am. Chem. Soc.* **2006**, *128*, 7756−7757.

(10) Liu, R.; Wu, D.; Liu, S.; Koynow, K.; Knoll, W.; Li, Q. An Aqueous Route to Multicolor Photoluminescent Carbon Dots Using Silica Spheres as Carriers. *Angew. Chem., Int. Ed.* **2009**, *48*, 4598−5601.

(11) Peng, H.; Travas-Sejdic, J. Simple Aqueous Solution Route to Luminescent Carbogenic Dots from Carbohydrates. *Chem. Mater.* **2009**, *21*, 5563−5565.

(12) Qian, Z.; Wang, Y.; Gao, Y.; Li, H.; Dai, T.; Liu, Y.; Huo, Q. Commercially Activated Carbon as the Source for Producing Multicolor Photoluminescent Carbon Dots by Chemical Oxidation. *Chem. Commun. (Cambridge, U. K.)* **2010**, *46*, 8812−8814.

(13) Wang, F.; Xie, Z.; Zhang, H.; Liu, C.-Y.; Zhang, Y.-G. Highly Luminescent Organosilane-Functionalized Carbon Dots. *Adv. Funct. Mater.* **2011**, *21*, 1027−1031.

(14) Zhu, S.; Zhang, J.; Tang, S.; Qian, C.; Wang, L.; Wang, H.; Liu, X.; Li, B.; Li, Y.; Yu, W.; Wang, X.; Sun, H.; Yang, B. Surface Chemistry Routes to Modulate the Photoluminescence of Graphene Quantum Dots: from Fluorescence Mechanism to Up-Conversion Bioimaging Applications. *Adv. Funct. Mater.* **2012**, *22*, 4732−4740.

(15) Qian, Z. S.; Ma, J. J.; Shan, X. Y.; Shao, L. X.; Zhou, J.; Chen, J. R.; Feng, H. Surface Functionalization of Graphene Quantum Dots with Small Organic Molecules from Photoluminescence Modulation to Bioimaging Applications: An Experimental and Theoretical Investigation. *RSC Adv.* **2013**, *3*, 14571−14579.

(16) Wang, R. X.; Zhu, R. X.; Zhang, D. J. Adsorption of Formaldehyde Molecule on the Pristine and Silicon-Doped Boron Nitride Nanotubes. *Chem. Phys. Lett.* **2008**, *467*, 131−135.

(17) Li, Y.; Zhao, Y.; Cheng, H. H.; Hu, Y.; Shi, G. Q.; Dai, L. M.; Qu, L. T. Nitrogen-Doped Graphene Quantum Dots with Oxygen-Rich Functional Groups. *J. Am. Chem. Soc.* **2012**, *134*, 15−18.

(18) Zhang, Y. Q.; Ma, D. K.; Zhuang, Y.; Zhang, X.; Chen, W.; Hong, L. L.; Yan, Q. X.; Yu, K.; Huang, S. M. One-Pot Synthesis of N-Doped Carbon Dots with Tunable Luminescence Properties. *J. Mater. Chem.* **2012**, *22*, 16714−16718.

(19) Xu, Y.; Wu, M.; Liu, Y.; Feng, X.; Yin, X.; He, X.; Zhang, Y. Nitrogen-Doped Carbon Dots: A Facile and General Preparation Method, Photoluminescence Investigation, and Imaging Applications. *Chem.—Eur. J.* **2013**, *19*, 2276−2283.

(20) Qian, Z. S.; Ma, J. J.; Shan, X. Y.; Feng, H.; Shao, L. X.; Chen, J. R. Highly Luminescent N-Doped Carbon Quantum Dots as An Effective Multifunctional Fluorescence Sensing Platform. *Chem.—Eur. J.* **2014**, *20*, 2254−2263.

(21) Chandra, S.; Patra, P.; Pathan, S. H.; Roy, S.; Mitra, S.; Layek, A.; Bhar, R.; Pramanik, P.; Goswami, A. Luminescent S-Doped Carbon Dots: An Emergent Architecture for Multimodal Applications. *J. Mater. Chem. B* **2013**, *1*, 2375−2382.

(22) Zhou, J.; Shan, X. Y.; Ma, J. J.; Gu, Y. M.; Qian, Z. S.; Chen, J. R.; Feng, H. Facile Synthesis of P-Doped Carbon Quantum Dots with Highly Efficient Photoluminescence. *RSC Adv.* **2014**, *4*, 5465−5468.

(23) Mauer, L. J.; Chernyshova, A. A.; Hiatt, A.; Deering, A.; Davis, R. Melamine Detection in Infant Formula Powder Using Near- and Mid-Infrared Spectroscopy. *J. Agric. Food Chem.* **2009**, *57*, 3974−3980.

6804

dx.doi.org/10.1021/am500403n | *ACS Appl. Mater. Interfaces* 2014, 6, 6797−6805

(24) Zhu, L.; Gamez, G.; Chen, H.; Chingin, K.; Zenobi, R. Rapid Detection of Melamine in Untreated Milk and Wheat Gluten by Untrasound-Assisted Extractive Electrospray Ionization Mass Spectrometry (EESI-MS). *Chem. Commun. (Cambridge, U. K.)* **2009**, *45*, 559−561.

(25) Wu, Y. N.; Zhao, Y. F.; Li, J. G.; Group, M. A. A Survey on Occurrence of Melamine and Its Analogues in Tainted Infant Formula in China. *Biomed. Environ. Sci.* **2009**, *22*, 95−99.

(26) Zeng, H.; Yang, R.; Wang, Q.; Li, J.; Qu, L. Determination of Melamine by Flow Injection Analysis Based on Chemiluminescence System. *Food Chem.* **2011**, *127*, 842−846.

(27) Sun, F.; Ma, W.; Xu, L.; Zhu, Y.; Liu, L.; Peng, C.; Wang, L.; Kuang, H.; Xu, C. Analytical Methods and Recent Developments in the Detection of Melamine. *Trends Anal. Chem.* **2010**, *29*, 1239−1249.

(28) Ai, K.; Liu, Y.; Lu, L. Hydrogen-Bonding Recognition-Induced Color Change of Gold Nanoparticles for Visual Detection of Melamine in Raw Milk and Infant Formula. *J. Am. Chem. Soc.* **2009**, *131*, 9496−9497.

(29) Wang, G.; Zhu, X.; Jiao, H.; Dong, Y.; Wu, X.; Li, Z. Oxidative Etching-Aggregation" of Silver Nanoparticles by Melamine and Electron Acceptors: An Innovative Route Toward Ultrasensitive and Versatile Functional Colorimetric Sensors. *Anal. Chim. Acta* **2012**, *747*, 92−98.

(30) Ding, N.; Yan, N.; Ren, C.; Chen, X. Colorimetric Determination of Melamine in Dairy Products by Fe_3O_4 Magnetic Nanoparticles-H_2O_2-ABTS Detection System. *Anal. Chem.* **2010**, *82*, 5897−5899.

(31) Liu, S.; Hu, J.; Zhang, H.; Su, X. $CuInS_2$ Quantum Dots-Based Fluorescence Turn off/on Probe for Detection of Melamine. *Talanta* **2012**, *101*, 368−373.

(32) Zhang, M.; Cao, X.; Li, H.; Guan, F.; Guo, J.; Shen, F.; Luo, Y.; Sun, C.; Zhang, L. Sensitive Fluorescent Detection of Melamine in Raw Milk Based on the Inner Filter Effect of Au Nanoparticles on the Fluorescence of CdTe Quantum Dots. *Food Chem.* **2012**, *135*, 1894−1900.

(33) Zheng, H.; Wang, Q.; Long, Y.; Zhang, H.; Huang, X.; Zhu, R. Enhancing the Luminescence of Carbon Dots with A Reduction Pathway. *Chem. Commun. (Cambridge, U. K.)* **2011**, *47*, 10650−10652.

(34) Zhu, S.; Meng, Q.; Wang, L.; Zhang, J.; Song, Y.; Jin, H.; Zhang, K.; Sun, H.; Wang, H.; Yang, B. Highly Photoluminescent Carbon Dots for Multicolor Patterning, Sensors and Bioimaging. *Angew. Chem., Int. Ed.* **2013**, *52*, 3953−3957.

(35) Moulder, J. F.; Stickle, W. F.; Sobel, P. E.; Bomben, K. D. *Handbook of X-Ray Photoelectron Spectroscopy-A Reference Book of Standard Spectra for Identification and Interpretation of XPS data*, 2nd ed; Perkin-Elmer Corporation: Eden Prairie, MN, 1992.

(36) Qian, Z. S.; Zhou, J.; Ma, J. J.; Shan, X. Y.; Chen, C. C.; Chen, J. R.; Feng, H. The Visible Photoluminescence Mechanism of Oxidized Multi-Walled Carbon Nanotubes: An Experimental and Theoretical Investigation. *J. Mater. Chem. C* **2013**, *1*, 307−314.

(37) Qian, Z. S.; Zhou, J.; Chen, J. R.; Wang, C.; Chen, C. C.; Feng, H. Nanosized N-Doped Graphene Oxide with Visible Fluorescence in Water for Metal Ion Sensing. *J. Mater. Chem.* **2011**, *21*, 17635−17637.

(38) Qian, Z. S.; Wang, C.; Du, G. H.; Zhou, J.; Ma, J. J.; Chen, J. R.; Feng, H. Multicolour Fluorescent Graphene Oxide by Cutting Carbon Nanotubes upon Oxidation. *CrystEngComm* **2012**, *14*, 4976−4979.

(39) Zhou, J.; Wang, C.; Qian, Z. S.; Chen, C. C.; Ma, J. J.; Du, G. H.; Chen, J. R.; Feng, H. Highly Efficient Fluorescent Multi-Walled Carbon Nanotubes Functionalized with Diamines and Amides. *J. Mater. Chem.* **2012**, *22*, 11912−11914.

(40) Hu, M.; Tian, J.; Lu, H.; Weng, L.; Wang, L. H_2O_2-Sensitive Quantum Dots for the Label-Free Detection of Glucose. *Talanta* **2010**, *82*, 997−1002.

(41) Yi, Y.; Deng, J.; Zhang, Y.; Li, H.; Yao, S. Label-Free Si Quantum Dots as Photoluminescence Probes for Glucose Detection. *Chem. Commun. (Cambridge, U. K.)* **2013**, *49*, 612−614.

(42) Xiang, D.; Zeng, G.; Zhai, K.; Li, L.; He, Z. Determination of Melamine in Milk Powder Based on the Fluorescence Enhancement of Au Nanoparticles. *Analyst* **2011**, *136*, 2837−2844.

(43) Guo, L.; Zhong, J.; Wu, J.; Fu, F.; Chen, G.; Chen, Y.; Zheng, X.; Lin, S. Sensitive Turn-on Fluorescent Detection of Melamine Based on Fluorescence Resonance Energy Transfer. *Analyst* **2011**, *136*, 1659−1663.

(44) Gao, F.; Ye, Q.; Cui, P.; Zhang, L. Efficient Fluorescence Energy Transfer System Between CdTe-Doped Silica Nanoparticles and Gold Nanoparticles for Turn-on Fluorescence Detection of Melamine. *J. Agric. Food Chem.* **2012**, *60*, 4550−4558.

(45) Wang, G.; Jiao, H.; Zhu, X.; Dong, Y.; Li, Z. Enhanced Fluorescence Sensing of Melamine Based on Thioglycolic Acid-capped CdS Quantum Dots. *Talanta* **2012**, *93*, 398−403.

6805

dx.doi.org/10.1021/am500403n | *ACS Appl. Mater. Interfaces* 2014, 6, 6797−6805